Chinese Chemical Letters 31 (2020) 1071–1077

Contents lists available at ScienceDirect

Chinese Chemical Letters

journal homepage: www.elsevier.com/locate/cclet

Review

Taming heterogeneous rhenium catalysis for the production of biomass-derived chemicals

Keiichi Tomishige*, Yoshinao Nakagawa, Masazumi Tamura

Department of Applied Chemistry, School of Engineering, Tohoku University, Miyagi 980-857, Japan

ARTICLE INFO

Article history:
Received 31 May 2019
Received in revised form 2 July 2019
Accepted 4 July 2019
Available online 4 July 2019

Keywords:
Rhenium
Oxidation state
Deoxydehydration
Hydrogenolysis
Hydrogenation

ABSTRACT

Rhenium is one of important components for heterogeneous catalysts, which has been recently used for the catalytic reactions related to the production of biomass-derived chemicals such as deoxydehydration of vicinal OH groups, C-O hydrogenolysis, and hydrogenation of carboxylic acids, and so on. Suitable oxidation state of Re as a catalytic active species is strongly dependent on the catalytic reactions. The control of the oxidation state of Re species on the catalysts is crucial on the catalyst development.

1. Introduction

Rhenium is able to have a variety of valences from zero to 7+ and this property can be connected to multifunctionality of Re catalysts. Metallic Re species has high activation ability of H_2 molecule, and Re with higher valence can have higher acidity, and so on. In addition, it is characteristic that Re has higher oxophilicity than other noble metals such as Pt, Ir. Possible multivalence property of Re can make the valence control difficult. Conversely, the control of the valence enables the extraction of functions on Re catalysts. A variety of Re catalysts has been recently applied to the reactions for the production of biomass-derived fuels and chemicals as mentioned in the reviews [1–10]. It has been known that the oxygen content of biomass-derived substrates (such as cellulose or sugars) is much higher than the value-added chemicals (such as a monomer for the production of plastics, resins). Building blocks in biomass refineries have been proposed and they also have high oxygen content [11]. Therefore, the reactions to decrease the oxygen contents become more and more important. The reactions include dehydration, reduction, and so on. In particular, reductants are necessary for the reduction and H_2 is one of the green reductants in terms of atom economy. Hydrodeoxygenation, C-O hydrogenolysis, deoxydehydration of biomass-related substrates with H_2 reductant can be included in the reduction. Here, the development of heterogeneous catalysts can increase the feasibility of the target process because of easy separation of the catalysts from the products and catalyst reusability. This short review introduces the development of heterogeneous Re catalysts for deoxydehydration of vicinal OH groups with H_2 reductant using high valence Re species, C-O hydrogenolysis using the combination of low valence Re species with noble metals, and hydrogenation of carboxylic acids using the combination of metallic Re with cationic Re species.

2. High valence Re species on oxide supports for deoxydehydration of vicinal OH groups with H_2 reductant

Deoxydehydration is the removal of vicinal OH groups to give carbon-carbon double bond as described below (Eq. 1).

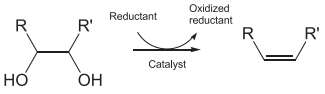

(1)

It has been reported that homogeneous Re(VII) complex such as $C_5Me_5ReO_3$ and CH_3ReO_3 catalyzes the deoxydehydration using PPh_3 and secondary alcohols as a reductant [12,13]. These Re complexes have low ability to activate H_2, and H_2 is not suitable reductant for the deoxydehydration. It has been proposed that the catalytic cycle consists of the reduction of Re(VII) to Re(V) with the 2-electron reductant (PPh_3 or secondary alcohols) and the successive oxidation of Re(V) in the Re diolate to give Re(VII) and the product with carbon-carbon double bond, which is regarded as the redox mechanism between Re(VII) and Re(V) as illustrated in Fig. 1.

* Corresponding author.
E-mail address: tomi@erec.che.tohoku.ac.jp (K. Tomishige).

https://doi.org/10.1016/j.cclet.2019.07.014

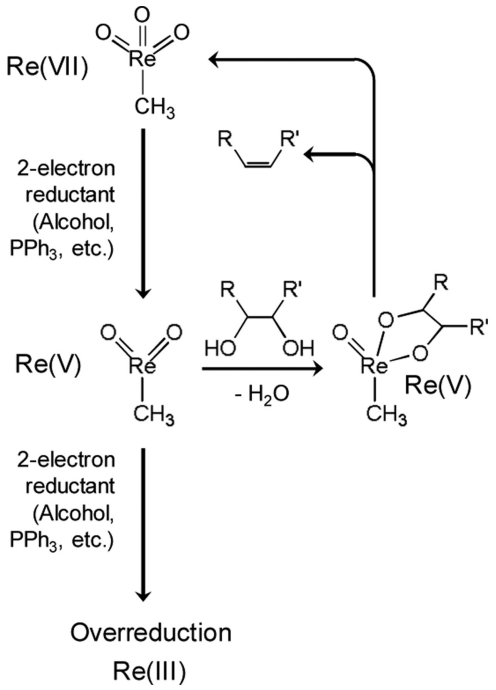

Fig. 1. Catalytic cycle of deoxydehydration of the substrates with vicinal OH groups using CH_3ReO_3 and 2-electron reductant.

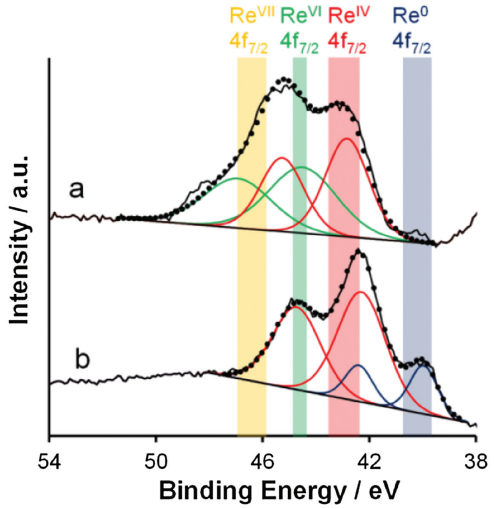

Fig. 2. XPS of reacted catalysts in Re 4f region. (a) ReO_x-Pd/CeO_2 after reaction (2 wt% Re, 0.3 wt% Pd, reaction temperature = 413 K, t = 4 h), (b) ReO_x-Pd/SiO_2 after reaction (2 wt% Re, 0.3 wt% Pd, reaction temperature = 413 K, t = 4 h). Raw XPS data (black solid line), calculated data (black dotted line). Reference: C 1s = 284.6 eV. Reprinted from with permission [16]. Copyright 2016, American Chemical Society.

There has been a previous report on the deoxydehydration of styrene glycol, 1,2-tetradecanediol, and (+)-diethyl tartrate with H_2 reductant to their products with carbon-carbon double bond in moderate-to-excellent yield over ReO_x/C [14]. The activity per Re amount on ReO_x/C in the deoxydehydration with H_2 reductant was clearly lower than that of homogeneous CH_3ReO_3 catalyst in deoxydehydration with 3-pentanol reductant. Our group has been developing more active heterogeneous Re catalysts for the deoxydehydration. Our approach for the catalyst development is the combination of high valent Re species fixed on oxides and noble metals with high H_2 activation ability, and we found that CeO_2 was much more effective support than carbon, SiO_2, ZrO_2, TiO_2, MgO, La_2O_3, and Al_2O_3 [15]. Regarding CeO_2-supported ReO_x catalyst (ReO_x/CeO_2), the modification effect of additive metals was investigated, and it is found that the Pd-added ReO_x/CeO_2 (ReO_x-Pd/CeO_2) showed high activity and selectivity to saturated product in the deoxydehydration + hydrogenation of 1,4-anhydroerythritol to tetrahydrofuran. The formation of saturated product can be due to high catalytic activity of Pd particles in hydrogenation of carbon-carbon double bond. The catalytic activity per Re amount of ReO_x-Pd/CeO_2 was clearly higher than that on CH_3ReO_3 in the deoxydehydration of 1,4-anhydroerythritol to 2,5-dihydrofuran [15,16]. An interesting behavior of ReO_x-Pd/CeO_2 is the effect of loading amount of Re. In the range of 0.5–2.0 wt% Re, the activity per g-cat increased with the increasing loading amount of Re. In the range of 2.0–10 wt%, the activity decreased with the decreasing loading amount of Re [15,16]. The optimum loading amount of Re is 2.0 wt%. The effect of loading amount on the catalytic activity and catalyst characterization indicates that monomeric Re species on CeO_2 is a catalytically active site in the deoxydehydration [16]. Only Re^{4+} and Re^{6+} species were detected in the XPS of highly active ReO_x-Pd/CeO_2 (2 wt% Re, 0.3 wt% Pd) after the reaction (Fig. 2), suggesting that the deoxydehydration proceeds by the redox of Re^{6+} and Re^{4+}. In contrast, in the XPS of ReO_x-Pd/SiO_2 (2 wt% Re, 0.3 wt% Pd) after the reaction, the presence of Re^{4+} and Re^0 species was verified (Fig. 2) [16]. It is clear that Re species tend to be reduced more deeply on ReO_x-Pd/SiO_2, which can be connected to the low catalytic activity due to overreduction of Re species. At the same time, the comparison of the results of CeO_2 and SiO_2 indicates that CeO_2 play a crucial role on the suppression of overreduction of Re species. In addition, in order to estimate the number of active site (monomeric Re species), the stoichiometric deoxydehydration of 1,2-hexanediol on the pre-reduced ReO_x-Pd/CeO_2 with various loading amounts of Re was carried out [16]. As a result, it is found that the ratio of the number of active Re species to total Re amount decreases with increasing the loading amount of Re. In the case of ReO_x-Pd/CeO_2 (2 wt% Re, 0.3 wt% Pd), the ratio is estimated to be about 0.4, meaning that almost half of Re species can be catalytically active site [16].

Another important behavior is the kinetics of deoxydehydration + hydrogenation of 1,4-anhydroerythritol to tetrahydrofuran. ReO_x-Pd/CeO_2 (2 wt% Re, 0.3 wt% Pd) showed almost zero reaction order with respect to H_2 pressure, indicating that the deoxydehydration of the Re-diolate species [16], which can be an intermediate from the studies on the homogeneous Re complexes, is the rate-determining step. The rate of the elementary steps including H_2 activation and the reduction of Re species, which can be strongly promoted by Pd, is much higher than that of deoxydehydration step. Pd has high H_2 activation ability to promote the reduction of Re species, at the same time, CeO_2 has the property for the strong suppression of the overreduction of Re species. Combination of the role of Pd and CeO_2 enables high performance of ReO_x-Pd/CeO_2.

A problem of ReO_x-Pd/CeO_2 catalyst is that unsaturated products in the deoxydehydration are not obtained. The key is the component to activate H_2 to promote the reduction of Re species on CeO_2 without the ability to hydrogenate carbon-carbon double bond in the unsaturated deoxydehydration product. As a result of metal survey as additive to ReO_x/CeO_2, we found that ReO_x-Au/CeO_2 gave unsaturated products such as allyl alcohol, 2,5-dihydrofuran and 1,3-butadiene in the deoxydehydration of glycerol, 1,4-anhydroerythritol, and erythritol with H_2 reductant, respectively [17,18]. Since Au nanoparticle with smaller size has higher catalytic activity, rather large Au particles (12 nm) exhibited high selectivity and high yield of unsaturated products, and the ReO_x-Au/CeO_2 catalysts are regarded as truly heterogeneous catalysts for the deoxydehydration with H_2 reductant [17,18]. The particle size of CeO_2 on ReO_x-Au/CeO_2 was estimated to be

about 8 nm, which is almost comparable to the size of Au (12 nm). In contrast, Pd metal particles on ReO_x-Pd/CeO_2 are highly dispersed. In the case of ReO_x-Au/CeO_2 (2 wt% Re, 0.3 wt% Au, particle size of Au = 12 nm), the number ratio of Au particles to CeO_2 particles is calculated to be 1:3000 [18]. The number of Au particles is very small compared to that of CeO_2 and Re species on CeO_2 (Fig. 3a), but the role of Au particles covers almost all the Re species on CeO_2, which can be explained by the spillover phenomenon of the hydrogen species formed on Au surface or Au-CeO_2 interface (Fig. 3b) [18].

This mechanism is also the case of ReO_x-Pd/CeO_2 catalysts, where hydrogen species can be supplied to Re species more rapidly than the case of ReO_x-Au/CeO_2. This can be because Pd metal particles have much higher dispersion than the case of Au and Pd has usually higher activity of H_2 activation than Au.

Here, the difference in the valences of the active Re species on CeO_2 and homogeneous Re complex such as CH_3ReO_3 is discussed. As shown in Fig. 1, CH_3ReO_3 has the two states of Re^{7+} and Re^{5+} during the deoxydehydration because 2-election reductant (secondary alcohol) and 2-electron oxidant (substrate with vicinal OH groups) are used for the catalytic reaction. In contrast, when H_2 is used as a reductant and the dissociated hydrogen species can be a real reductant on ReO_x-M/CeO_2 catalyst, the valence of Re species can be changed step by step as shown in Fig. 4 [18]. An important point is that the overreduction of Re species from Re^{4+} can be suppressed by the presence of CeO_2 support. This mechanism is unclear at present, however, further investigation such as DFT calculation is necessary [19].

Fig. 5 shows the applicability of ReO_x-Au/CeO_2 for deoxydehydration and ReO_x-Pd/CeO_2 for deoxydehydration + hydrogenation using H_2 reductant, which can contribute to the production of biomass-derived chemicals [15–18,20–23].

3. Low valent Re species on metal surface for C–O hydrogenolysis

Our group reported that Rh-ReO_x/SiO_2 showed much higher catalytic activity in the C–O hydrogenolysis of glycerol in 2009, although the selectivity to 1,3-propanediol was not high [24]. Effective combination of noble metals with ReO_x is a little limited, and Rh-ReO_x and Ir-ReO_x showed high catalytic performance in the C–O hydrogenolysis [25–47]. The chemical state of Re species on noble-metal-ReO_x based catalysts has been investigated. The structural change of Rh-ReO_x/SiO_2 (4 wt% Rh, Re/Rh = 0.5) during the temperature programmed reduction (TPR) with H_2 was investigated using *in situ* Re L_3-edge and Rh *K*-edge quick-scanning X-ray absorption fine structure in the temperature range of room temperature to 600 K [31]. Rh-ReO_x/SiO_2 (4 wt% Rh, Re/Rh = 0.5) showed high catalytic activity and selectivity in the C–O hydrogenolysis of tetrahydrofurfuryl alcohol to 1,5-pentanediol [25]. The valence of Rh and Re on Rh-ReO_x/SiO_2 (Re/Rh = 0.5) was determined individually from the coordination number of Rh–O bond in the Rh *K*-edge EXAFS analysis and the chemical shift of the binding energy in the Re L_3-edge XANES analysis. It is concluded that the reduction of Re species followed that of Rh, although Rh-ReO_x/SiO_2 gave single peak in the TPR profile [31]. An interesting point is that the average valence of Re is maintained to be around 2+ in the temperature range of 373–600 K, and the further reduction of Re cation to metallic Re can be suppressed, although the reduction of Re is strongly promoted by the presence of Rh. At the same time, the Re L_3-edge EXAFS analysis indicates that the Re-O, Re-Rh, and Re-Re bonds are detected on Rh-ReO_x/SiO_2 (Re/Rh = 0.5) [31]. In particular, the bond length of Re-Rh and Re-Re bonds is about 0.265 nm and 0.270 nm, respectively. These bond lengths are very close to the sum of metal bond radius of Rh and Re, indicating the direct bond between Re atom and Rh atom. Based on the average valence of Re (~2+), partially oxidized Re species can be located on the surface of Rh metal surface [31]. Considering the coordination numbers of Re-Rh, Re-Re and Re-O bonds, 2-dimensional clusters of Re oxides in low valence can be formed on the surface on Rh metal particles [31].

The structure of Pt-ReO_x/SiO_2 (2 wt% Pt, Re/Pt = 0.2 and 0.5) was also examined by X-ray absorption spectroscopy [48]. The Re L_3-edge EXAFS analysis indicates that the Re-O, Re-Pt, and Re-Re bonds are detected on Pt-ReO_x/SiO_2 catalysts. The bond length of Re-Pt and Re-Re bonds is about 0.275 nm and 0.268 nm, respectively. These bond lengths are very close to the sum of metal bond radius of Re and Pt, indicating the direct bond between Re atom and Pt atom. Based on the average valence of Re (~3+), partially oxidized Re species can be located on the surface of Pt metal surface. Considering the coordination numbers of Re-Pt, Re-Re and Re-O bonds, 2-dimensional clusters of Re oxides in low valence can be also formed on the surface on Pt metal particles [48]. As a result, the structure of ReO_x on Rh and Pt metal surface can be similar. On the other hand, the catalytic activity of Rh-ReO_x/SiO_2 and Pt-ReO_x/SiO_2 in the C-O hydrogenolysis of glycerol and tetrahydrofurfuryl alcohol was very different regardless of similar structure [26]. According to the kinetics analysis of the C-O hydrogenolysis of tetrahydrofurfuryl alcohol to 1,5-pentanediol, the reaction order with respect to H_2 pressure is first, indicating that the reaction of hydrogen species can be rate-determining step [29]. The activity difference may be explained by the ability to form the active hydrogen species such as hydride, however, further investigation is necessary for the explanation supported by DFT studies and so on.

The Ir-ReO_x/SiO_2 (4 wt% Ir, Re/Ir = 1, 2) showed high catalytic activity of C-O hydrogenolysis of glycerol, and it is characteristic

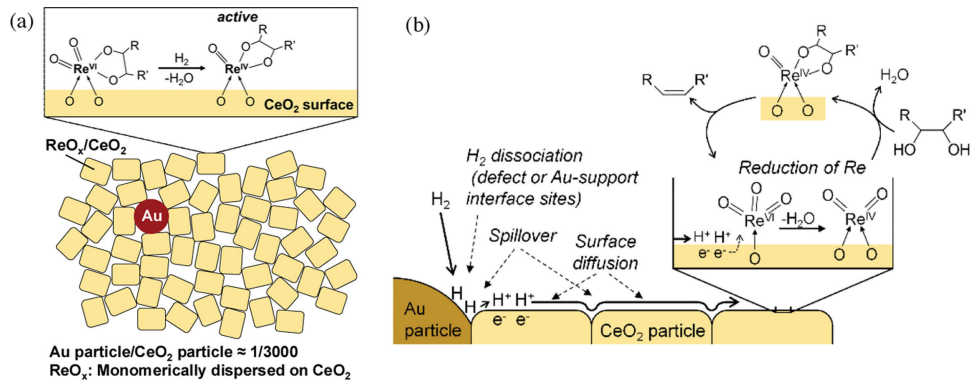

Fig. 3. Illustration of each component of ReO_x-Au/CeO_2 (2 wt% Re, 0.3 wt% Au, particle size of Au: 12 nm, size of CeO_2: 8 nm) (a), and the model scheme of H_2 activation and spillover from Au to ReO_x *via* CeO_2 (b). Reprinted from with permission [18]. Copyright 2018, American Chemical Society.

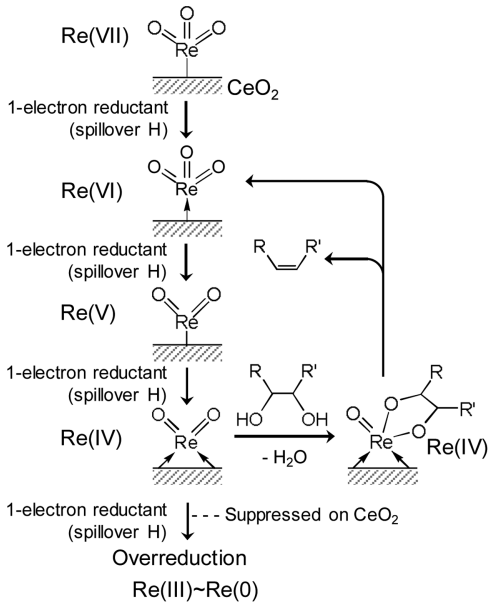

Fig. 4. Catalytic cycle of deoxydehydration of the substrates with vicinal OH groups using ReO_x-M/CeO_2 (M = Pd, Au) and H_2 reductant.

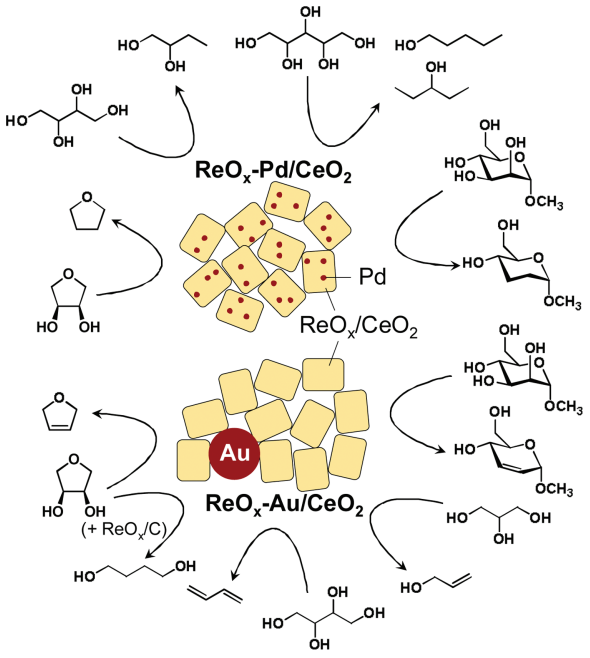

Fig. 5. Example of application of ReO_x-Au/CeO_2 for deoxydehydration and ReO_x-Pd/CeO_2 for deoxydehydration + hydrogenation using H_2 reductant.

that Ir-ReO_x/SiO_2 exhibited higher selectivity to 1,3-propanediol than Rh-ReO_x/SiO_2 [32,33]. The structural change of Ir-ReO_x/SiO_2 (4 wt% Ir, Re/Ir = 1) during TPR with H_2 was also investigated using *in situ* Ir and Re L_3-edge quick-scanning X-ray absorption fine structure in the temperature range from room temperature to 900 K [37]. The valence of Ir and Re on Ir-ReO_x/SiO_2 (4 wt% Ir, Re/Ir = 1) was determined individually from the coordination number of Ir–O or Re-O bond in the EXAFS analysis and the chemical shift of the binding energy in the Ir and Re L_3-edge XANES analysis [37]. It is concluded that Ir and Re species on Ir-ReO_x/SiO_2 (4 wt% Ir, Re/Ir = 1) are reduced almost simultaneously to metallic Ir and low valence Re (about +2) [37]. An interesting point is that the average valence of Re is maintained to be around 2+ in the

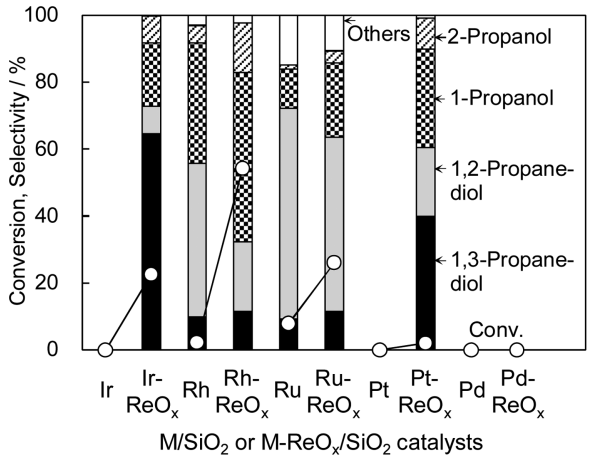

Fig. 6. Hydrogenolysis of glycerol over M/SiO_2 and M-ReO_x/SiO_2 (4 wt% M, Re/M = 0.25) catalysts. Conditions: glycerol 4 g, water 2 g, catalyst (reduced at 473 K (for Rh-ReO_x/SiO_2: 393 K)) 0.15 g, H_2SO_4 H^+/Re = 1, H_2 8 MPa, 393 K, 12 h [33].

temperature range of 485–600 K, and the further reduction of Re cation to metallic Re can be suppressed, although the reduction of Re is strongly promoted by the presence of Ir [37]. The coordination number of Re-Ir or Re bond increased clearly at higher reduction temperature (>600 K). The Re L_3-edge EXAFS analysis indicates that the Re-O, Re-Ir or Re bonds are detected on Ir-ReO_x/SiO_2 (4 wt% Ir, Re/Ir = 1) [37]. In particular, the length of Re-Ir or Re bond is about 0.272–0.274 nm, which is also close to the sum of metal bond radius of Ir and Re, indicating the direct bond [37]. Based on the average valence of Re (~2+), coordination numbers and other characterization results, we propose that the Ir metal particles covered with 3-dimensional clusters of low valence Re oxides [37].

On the three catalysts of M-ReO_x/SiO_2 (M = Rh, Pt, Ir) catalysts, it is common that small clusters of low valent Re species is formed on the surface of metal particles, which can be explained by the higher oxygen affinity of Re than that of Rh, Pt and Ir. However, the catalytic performance in the C-O hydrogenolysis is strongly dependent on noble metals. The activity of Rh-ReO_x/SiO_2 and Ir-ReO_x/SiO_2 in the glycerol hydrogenolysis was much higher than that of Pt-ReO_x/SiO_2 (Fig. 6) [33].

At present, this can be interpreted by the formation of active hydrogen species (such as hydride) on Rh-Re and Ir-Re interface from the heterolytic dissociation of H_2. In contrast, high selectivity to 1,3-propanediol in the glycerol hydrogenolysis can be related to the structure of Re oxide clusters, and 3-dimensional clusters are more favorable than 2-dimensional ones [8]. The rate-determining step can be the S_N2-like attack of hydride at the interface of Rh-Re or Ir-Re to the adsorbed glycerol species on ReO_x clusters as shown in Fig. 7. The presence of Re species at the second layer of the 3-dimensional clusters stabilize the adsorbed glycerol species giving 1,3-propanediol. The mechanism of glycerol hydrogenolysis on Rh-ReO_x and Ir-ReO_x have been recently studied in a theoretical approach, and further investigation is necessary for the deeper understanding [49]. Rh-ReO_x and Ir-ReO_x catalysts are applicable to the selective and deep C-O hydrogenolysis of various substrates and selective hydrogenation of C = O in unsaturated aldehyde and so on (Fig. 8) [24–48,50,51].

The additive effect of Ni, Co, Zn, Cu, and Ag to Ir-ReO_x/SiO_2 (Re/Ir = 2) was investigated in the glycerol hydrogenolysis [41], and the addition of the above components decreased the catalytic activity of Ir-ReO_x/SiO_2 drastically. The reason of the activity decrease is not elucidated in detail, however, the above additives can be regarded as a poison for the hydrogen activation on Ir-ReO_x/SiO_2. For example, the above components have lower reducibility than noble metals, and they also tend to leach to the aqueous solution and

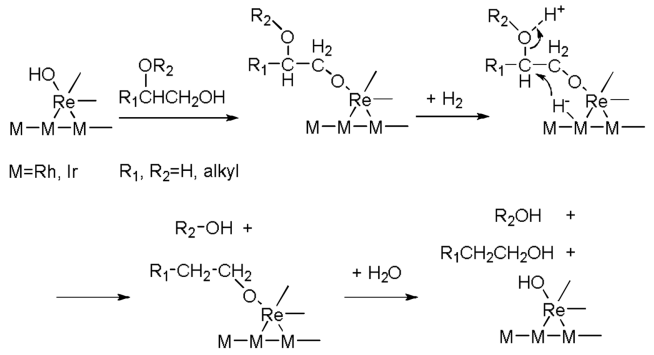

Fig. 7. Proposed mechanism of the hydrogenolysis of glycerol and related substrates over ReO_x-modified Rh or Ir catalysts.

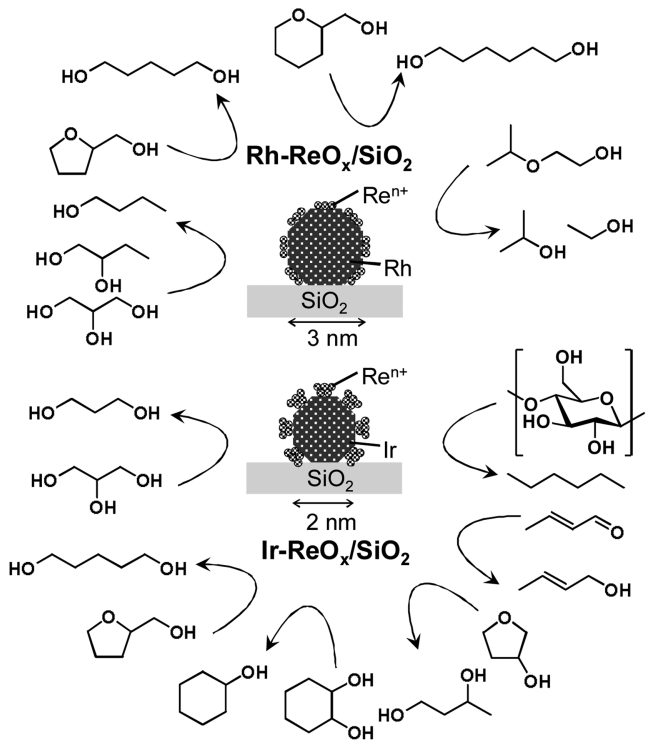

Fig. 8. Hydrogenation or hydrogenolysis catalyzed by Rh-ReO_x/SiO_2 and Ir-ReO_x/SiO_2.

the re-deposition on the catalyst surface. Judging from these results and behaviors, it is a challenging task to substitute noble metals with non-noble metals in the C-O hydrogenolysis using the proposed reaction mechanism.

4. Re metal particle modified with low valent ReO_x species for hydrogenation of carboxylic acid

In the X-ray absorption spectroscopic studies of Rh-ReO_x/SiO_2, the structural change of ReO_x/SiO_2 (3.6 wt% Re) catalyst during TPR with H_2 was also investigated as a reference [31]. The reduction of ReO_x/SiO_2 proceeded above 600 K, which was much higher temperature than that in the presence of noble metals [31]. After the reduction at 873 K, the XRD peaks assigned to Re metal were detected clearly, and the particle size of Re metal was estimated to be 9.5 nm [31]. Assuming all the Re species are reduced to metallic state, the dispersion is calculated to be 0.14. At the same time, the coordination number of Re-Re bond is determined to be 10.9,

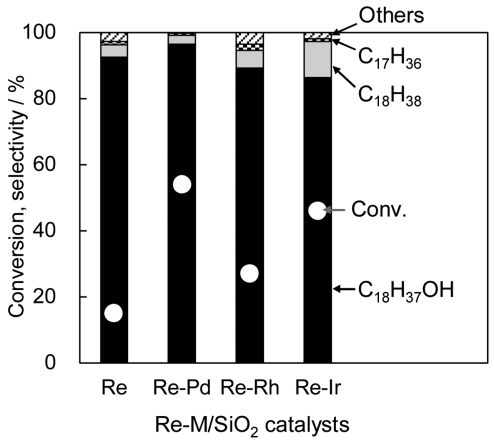

Fig. 9. Hydrogenation of stearic acid over Re-M/SiO_2 catalysts. Conditions: stearic acid 1 g, 1,4-dioxane 19 g, catalyst (14 wt% Re, M/Re = 0 or 1/8) 0.1 g, H_2 8 MPa, 413 K, 4 h [52].

which also supported the formation of rather large Re metal particles [31]. On the other hand, the dispersion from the amount of CO adsorption on ReO_x/SiO_2 was measured to be <0.01, which is much lower than that from XRD, indicating that the CO adsorption is strongly suppressed [31]. One explanation for this disagreement in the dispersion is covering Re metal surface with low valent Re species. The presence of low valent Re species is supported by the non-zero average valence from XANES analysis (0∼+1) and the presence of Re-O bond from the EXAFS analysis [31]. It is characteristic that high oxophilicity of Re element enables the coexistence of metallic and cationic states, which is connected to unique catalytic properties of Re. On the other hand, the coexistence of various states of Re species makes the structural elucidation difficult. We discussed and proposed the structure of Re-Pd/SiO_2, where Re is the main catalytically active component and Pd is the cocatalyst, for the hydrogenation of carboxylic acid. This is supported by the results that Pd/SiO_2 showed almost no activity, and monometallic Re/SiO_2 showed some activity, and bimetallic Re-Pd/SiO_2 showed clearly higher activity than Re/SiO_2 at the same Re loading amount [52–54]. In addition, the combination of Pd with Re (Re-Pd) is more suitable to that of Re-Rh and Re-Ir from the viewpoint of the target product yield (alcohols), which can be related to lower reactivity of the target products (alcohols) on Pd-ReO_x than that on Rh-ReO_x and Ir-ReO_x in the C-O hydrogenolysis (Fig. 9).

Another important factor for high catalytic performance in the hydrogenation of carboxylic acids over Re-Pd/SiO_2 catalysts is the reduction method (Fig. 10) [53]. In our case, we compared the three reduction pretreatment methods: gas phase reduction, *in-situ* liquid phase reduction, *ex-situ* liquid phase reduction. Here, "*in-situ*" means liquid phase containing both substrate (carboxylic acid) and solvent (1,4-dioxane), and "*ex-situ*" means liquid phase containing only the solvent, and in all cases, H_2 is the reductant.

As shown in Fig. 10, gas phase reduction at 473 K is not suitable on both catalysts. According to the TPR profiles, the reduction of Re/SiO_2 needs higher temperature than Re-Pd/SiO_2, therefore, we also tested the gas phase reduction at 773 K, Re/SiO_2 showed low catalytic activity. On the other hand, Re/SiO_2 with *in-situ* liquid phase reduction showed rather high catalytic activity. Both Re-Pd/SiO_2 with *in-situ* and *ex-situ* liquid phase reduction showed much higher activity than that with gas phase reduction and ReO_x/SiO_2 with *in-situ* liquid phase reduction [53].

In the XRD patterns of the catalysts after the catalytic use, which were measured without exposing the samples to air, the peaks assigned to Re hcp metal and Re fcc metal are detected, Based on the area of peaks and the dispersion estimated from the

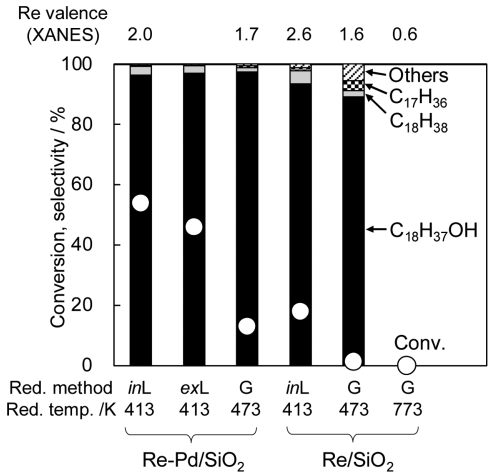

Fig. 10. Effect of reduction method on hydrogenation of stearic acid over Re-Pd/SiO_2 catalysts. Conditions: stearic acid 1 g, 1,4-dioxane 19 g, catalyst (14 wt% Re, Pd/Re = 0 or 1/8) 0.1 g, H_2 8 MPa, 413 K, 4 h. For reduction method, "*in*L", "*ex*L" and "G" means *in situ* reduction in liquid phase, *ex situ* reduction in liquid phase, and gas phase reduction, respectively [53].

peak width, the number of Re metal atoms on the used catalysts can be estimated by the sum of (the area) x (the dispersion), which is called the effective XRD area. Fig. 11 shows the relation between this effective XRD area and conversion rate of the hydrogenation of stearic acid [53]. Regarding Re-Pd catalysts with the *in-situ* liquid-phase reduction, the conversion rate can be related to effective XRD area, however, the conversion rate on Re-Pd and Re catalysts with gas phase reduction was clearly lower than that on Re-Pd catalysts with the *in-situ* liquid-phase reduction, suggesting that the surface structure or property of the catalysts with gas phase reduction is different from that of the catalysts with *in-situ* liquid-phase reduction.

According to the Re L_3-edge XANES analysis, the average valence of Re on the catalysts with gas phase reduction is relatively lower than that on the catalysts with *in-situ* liquid phase reduction (Fig. 10). The combination of the characterization results enables the

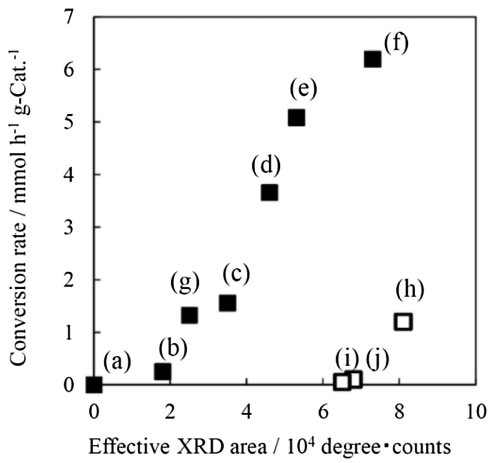

Fig. 11. Conversion rate of stearic acid hydrogenation as a function of effective XRD area of Pd/SiO_2 (1 wt% Pd), Re-Pd/SiO_2 (1 wt% Pd) and Re/SiO_2 (14 wt% Re) catalysts. (a) Pd (*in*L, 413, Reaction), (b) Re-Pd (*in*L, 413, Reaction) (Re/Pd = 2), (c) Re-Pd (*in*L, 413, Reaction) (Re/Pd = 4), (d) Re-Pd (*in*L, 413, Reaction) (Re/Pd = 6), (e) Re-Pd (*in*L, 413, Reaction) (Re/Pd = 8), (f) Re-Pd (*in*L, 413, Reaction) (Re/Pd = 12), (g) Re (*in*L, 413, Reaction), (h) Re-Pd (G, 473) (Re/Pd = 8), (i) Re (G, 473), (j) Re (G, 473). Effective XRD area = XRD area × Re dispersion. "Reaction" in the parenthesis represents the sample after the reaction of stearic acid hydrogenation. Reprinted with permission [53]. Copyright 2015, American Chemical Society.

estimation of the ratio of $(Re^{3+}+Re^{4+})/(Re^0{}_s+Pd^0{}_s)$ on Re-Pd/SiO_2 (Re = 14 wt%, Pd = 1 wt%, Re/Pd = 8), where $M^0{}_s$ represents the number of metal atom on the surface of the metal particles, and it is the degree of the coverage of Re cations on the metal surface. Highly active Re-Pd (*ex*L, 413) in the hydrogenation of succinic acid and Re-Pd (*in*L, 413) in the hydrogenation of stearic acid gave 0.9 and 2.2 of $(Re^{3+}+Re^{4+})/(Re^0{}_s+Pd^0{}_s)$, respectively, after the reaction. In contrast, high value (7.9) and very low value (0.4) of $(Re^{3+}+Re^{4+})/(Re^0{}_s+Pd^0{}_s)$ over Re-Pd (*in*L, 413) and Re-Pd (G, 473) with lower catalytic activity were observed. From the comparison, the medium coverage of Re cations on the metal surface can be connected to high catalytic activity of the hydrogenation of carboxylic acids, which suggests that the interaction between Re cations and Re (or Pd) metal surface can be the catalytically active site.

5. Conclusions

High valent rhenium species stabilized on CeO_2 modified with Pd and Au catalyzed the deoxydehydration of various substrates with vicinal OH groups with H_2 reductant as heterogeneous catalysts. Medium valent rhenium species are stabilized on the surface of Rh and Ir metal particles, and the interface of Re cations and the metal surface can be a catalytically active site for the C-O hydrogenolysis of various biomass-related substrates. In addition, part of rhenium on SiO_2 at high loading amount was reduced to metallic state to give Re metal particles and cationic Re species partially covered the surface of Re metal particles. Reduction conditions can influence the reduction degree of Re species and the coverage ratio of cationic Re species. The Re-Pd/SiO_2 with medium coverage ratio of cationic Re species is suitable to the catalysts for hydrogenation of carboxylic acids. The control or stabilization of specific oxidation states of Re species will be connected to the development of catalysts with high performance.

References

[1] Y. Nakagawa, K. Tomishige, Catal. Sci. Technol. 1 (2011) 179–190.
[2] Y. Nakagawa, K. Tomishige, Catal. Today 195 (2012) 136–143.
[3] Y. Nakagawa, M. Tamura, K. Tomishige, ACS Catal. 3 (2013) 2655–2668.
[4] Y. Nakagawa, M. Tamura, K. Tomishige, J. Mater. Chem. A 2 (2014) 6688–6702.
[5] K. Tomishige, M. Tamura, Y. Nakagawa, Chem. Rec. 14 (2014) 1041–1054.
[6] Y. Nakagawa, S. Liu, M. Tamura, K. Tomishige, ChemSusChem 8 (2015) 1114–1132.
[7] Y. Nakagawa, M. Tamura, K. Tomishige, Catal. Surv. Asia 19 (2015) 249–256.
[8] K. Tomishige, Y. Nakagawa, M. Tamura, Green Chem. 19 (2017) 2876–2924.
[9] Y. Nakagawa, M. Tamura, K. Tomishige, Res. Chem. Intermed. 44 (2018) 3879–3903.
[10] Y. Nakagawa, M. Tamura, K. Tomishige, Fuel Proc. Technol. 193 (2019) 404–422.
[11] J.J. Bozell, G.R. Petersen, Green Chem. 12 (2010) 539–554.
[12] G.K. Cook, M.A. Andrews, J. Am. Chem. Soc. 118 (1996) 9448–9449.
[13] M. Shiramizu, F.D. Toste, Angew. Chem. Int. Ed. 51 (2012) 8082–8086.
[14] A.L. Denning, H. Dang, Z. Liu, K.M. Nicholas, F.C. Jentoft, ChemCatChem 5 (2013) 3567–3570.
[15] N. Ota, M. Tamura, Y. Nakagawa, K. Okumura, K. Tomishige, Angew. Chem. Int. Ed. 54 (2015) 1897–1900.
[16] N. Ota, M. Tamura, Y. Nakagawa, K. Okumura, K. Tomishige, ACS Catal. 6 (2016) 3213–3226.
[17] S. Tazawa, N. Ota, M. Tamura, et al., ACS Catal. 6 (2016) 6393–6397.
[18] Y. Nakagawa, S. Tazawa, T. Wang, et al., ACS Catal. 8 (2018) 584–595.
[19] Y. Xi, W. Yang, S.C. Ammal, et al., Catal. Sci. Technol. 8 (2018) 5750–5762.
[20] T. Wang, S. Liu, M. Tamura, et al., Green Chem. 20 (2018) 2547–2557.
[21] M. Tamura, N. Yuasa, J. Cao, Y. Nakagawa, K. Tomishige, Angew. Chem. Int. Ed. 57 (2018) 8058–8062.
[22] J. Cao, M. Tamura, Y. Nakagawa, K. Tomishige, ACS Catal. 9 (2019) 3725–3729.
[23] T. Wang, M. Tamura, Y. Nakagawa, K. Tomishige, ChemSusChem (2019), doi: http://dx.doi.org/10.1002/cssc.201900900.
[24] A. Shimao, S. Koso, N. Ueda, et al., Chem. Lett. 38 (2009) 540–541.
[25] S. Koso, I. Furikado, A. Shimao, et al., Chem. Commun. (2009) 2035–2037.
[26] Y. Shinmi, S. Koso, T. Kubota, Y. Nakagawa, K. Tomishige, Appl. Catal. B 94 (2010) 318–326.
[27] K. Chen, S. Koso, T. Kubota, Y. Nakagawa, K. Tomishige, ChemCatChem 2 (2010) 547–555.
[28] Y. Amada, S. Koso, Y. Nakagawa, K. Tomishige, ChemSusChem 3 (2010) 728–736.
[29] S. Koso, Y. Nakagawa, K. Tomishige, J. Catal. 280 (2011) 221–229.

[30] S. Koso, H. Watanabe, K. Okumura, Y. Nakagawa, K. Tomishige, Appl. Catal. B 111–112 (2012) 27–37.
[31] S. Koso, H. Watanabe, K. Okumura, Y. Nakagawa, K. Tomishige, J. Phys. Chem. C 116 (2012) 3079–3090.
[32] Y. Nakagawa, Y. Shinmi, S. Koso, K. Tomishige, J. Catal. 272 (2010) 191–194.
[33] Y. Amada, Y. Shinmi, S. Koso, et al., Appl. Catal. B 105 (2011) 117–127.
[34] Y. Nakagawa, X. Ning, Y. Amada, K. Tomishige, Appl. Catal. A 433–434 (2012) 128–134.
[35] K. Chen, K. Mori, H. Watanabe, Y. Nakagawa, K. Tomishige, J. Catal. 243 (2012) 171–183.
[36] Y. Amada, H. Watanabe, Y. Hirai, et al., ChemSusChem 5 (2012) 1991–1999.
[37] Y. Amada, H. Watanabe, M. Tamura, et al., J. Phys. Chem. C 116 (2012) 23503–23514.
[38] K. Chen, M. Tamura, Z. Yuan, Y. Nakagawa, K. Tomishige, ChemSusChem 6 (2013) 613–621.
[39] Y. Nakagawa, K. Mori, K. Chen, et al., Appl. Catal. A 468 (2013) 418–425.
[40] S. Liu, Y. Amada, M. Tamura, Y. Nakagawa, K. Tomishige, Green Chem. 16 (2014) 617–626.
[41] M. Tamura, Y. Amada, S. Liu, et al., J. Mol. Catal. A 388–389 (2014) 177–187.
[42] S. Liu, Y. Amada, M. Tamura, Y. Nakagawa, K. Tomishige, Catal. Sci. Technol. 4 (2014) 2535–2549.
[43] S. Liu, M. Tamura, Y. Nakagawa, K. Tomishige, ACS Sustain. Chem. Eng. 2 (2014) 1819–1827.
[44] S. Liu, Y. Okuyama, M. Tamura, et al., ChemSusChem 8 (2015) 628–635.
[45] S. Liu, Y. Okuyama, M. Tamura, et al., Green Chem. 18 (2016) 165–175.
[46] S. Liu, M. Tamura, Z. Shen, et al., Catal. Today 303 (2018) 106–116.
[47] L. Liu, S. Kawakami, Y. Nakagawa, M. Tamura, K. Tomishige, Appl. Catal. B 256 (2019) 117775.
[48] T. Ebashi, Y. Ishida, Y. Nakagawa, et al., J. Phys. Chem. C 114 (2010) 6518–6526.
[49] J.J. Varghese, L. Cao, C. Robertson, et al., ACS Catal. 9 (2019) 485–503.
[50] M. Tamura, K. Tokonami, Y. Nakagawa, K. Tomishige, Chem. Commun. 49 (2013) 7034–7036.
[51] M. Tamura, K. Tokonami, Y. Nakagawa, K. Tomishige, ACS Catal. 6 (2016) 3600–3609.
[52] Y. Takeda, Y. Nakagawa, K. Tomishige, Catal. Sci. Technol. 2 (2012) 2221–2223.
[53] Y. Takeda, M. Tamura, Y. Nakagawa, K. Okumura, K. Tomishige, ACS Catal. 5 (2015) 7034–7047.
[54] Y. Takeda, M. Tamura, Y. Nakagawa, K. Okumura, K. Tomishige, Catal. Sci. Technol. 6 (2016) 5668–5683.